

RSC Advances



This is an *Accepted Manuscript*, which has been through the Royal Society of Chemistry peer review process and has been accepted for publication.

Accepted Manuscripts are published online shortly after acceptance, before technical editing, formatting and proof reading. Using this free service, authors can make their results available to the community, in citable form, before we publish the edited article. This *Accepted Manuscript* will be replaced by the edited, formatted and paginated article as soon as this is available.

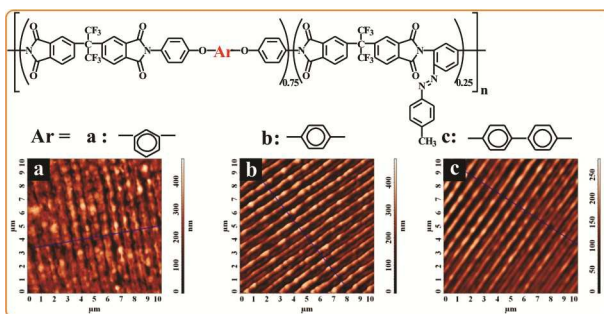
You can find more information about *Accepted Manuscripts* in the [Information for Authors](#).

Please note that technical editing may introduce minor changes to the text and/or graphics, which may alter content. The journal's standard [Terms & Conditions](#) and the [Ethical guidelines](#) still apply. In no event shall the Royal Society of Chemistry be held responsible for any errors or omissions in this *Accepted Manuscript* or any consequences arising from the use of any information it contains.

Properties of some azo-copolyimide thin films used in formation of photoinduced surface relief gratings

Ion Sava, Ada Burescu, Iuliana Stoica, Valentina Musteata, Mariana Cristea, Ilarion Mihaila, Valentin Pohoata and Ionut Topala

The patterning of the free standing azo-copolyimide films under different irradiation conditions led to the uniform surface relief gratings.



Cite this: DOI: 10.1039/c0xx00000x

www.rsc.org/xxxxxx

ARTICLE TYPE

Properties of some azo-copolyimide thin films used in formation of photoinduced surface relief gratings

Ion Sava^{1*}, Ada Burescu¹, Iuliana Stoica^{1,3}, Valentina Musteata¹, Mariana Cristea¹, Ilarion Mihaila², Valentin Pohoata² and Ionut Topala²

¹“Petru Poni” Institute of Macromolecular Chemistry, Aleea Gr. Ghica Voda 41A, Iasi 700553, Romania; Email: isava@icmpp.ro

²“Alexandru Ioan Cuza” University of Iasi, Faculty of Physics, Plasma Advanced Research Center (IPARC), Bd. Carol I no. 11, Iasi, 700506, Romania

³ University POLITEHNICA of Bucharest, Str. Gheorghe Polizu, Sector 1, Bucharest 011061, Romania

Received (in XXX, XXX) Xth November 2014, Accepted Xth XXXXXXXXXX 20XX

DOI: 10.1039/b000000x

Abstract. Thin free standing films have been obtained by casting from dimethylacetamide solutions of some azo-copolyimides. The dynamo-mechanical and dielectric properties, and the effect of the chemical structure of polymers of the physical properties are investigated. The incorporation of substituted azobenzene groups and hexafluoroisopropylidene units in the macromolecular chain allowed the patterning of the materials under different irradiation conditions. The azo-copolyimide thin films showed high thermal stability, low dielectric constant, good dynamo-mechanical characteristics and uniform surface relief gratings.

15

1. Introduction

For a broad class of aromatic azo-compounds, azobenzene, with two phenyl rings separated by an azo (-N=N-) bond is considered as the parent molecule. These chromophores are versatile molecules and have drawn much attention in fundamental and applied research areas. Due to their capacity of responding spontaneously to external stimuli by light, the azo-compounds can be considered as “smart materials”. The exposure to the linearly polarized light of an appropriate wavelength results in a directed reorientation of photochromic group’s perpendicular to the electric field vector of the incident light. This process takes place with multiple reversible *trans* to *cis* photoisomerization, which leads to the generation of photoinduced optical anisotropy. The photoinduced optical anisotropy is a key for many applications including optical devices for storage, processing, displaying, and transfer of optical information.¹⁻¹⁰

The large-scale mass transport of the polymer chains can take place in the case of polymers which contain azobenzene units due to the cyclic photoisomerization of azobenzene-based groups. This behavior can be observed as a surface relief grating (SRG).¹¹⁻¹³ These kinds of polymers which can be suitable for the efficient SRG formation reveal many possible applications

mostly in photonics and for micro and nanoscale processing technologies in microelectronics.¹³

Due to the fact that azo-polymers are promising materials for many practical applications, further improvement of their performance is necessary. Thus, long-term chemical and orientational stabilities is still required at the high temperatures of their use.⁶ To obtain stable photonic structures or long-term storage optical devices, azo-polymers with a good thermal stability and high T_g values are desirable. Photoinduced optical anisotropy and the formed surface relief gratings are relatively stable below the azo-polymer glass transition temperature (T_g) and are erasable by laser or heating.⁶ Polymers with such properties have shown potential technological applications such as optical information storage and processing, optical switching devices, holographic gratings, nano-manipulation and so on.^{11,14}

These requirements meet polyimides (PI) which are an important class of high-performance polymers useful in a variety of applications. Aromatic polyimides are unique due to their optical and thermal stability, high glass transition temperature, chemical resistance, electrical characteristics, low susceptibility to the laser damage, low dielectric constant value, toughness, and

dimensional stability. These excellent properties led to broad spectrum of potential applications of these polymers.¹⁵⁻¹⁷

Polyimides with azobenzene derivatives have already been investigated for photoinduced alignment in a liquid crystal display,¹⁸ photomechanical response materials¹⁹⁻²² and for holographic recording.²³⁻²⁵ The most of the synthesized azo-polyimides contain covalently attached chromophores mainly as side-groups of the polymer backbone²⁶⁻³³ and only few papers report the preparation and characterization of polyimides with azobenzene derivatives placed in the main chain.^{21,22,34-36}

It was expected that the incorporation of the substituted azobenzene units, connected in a special way (a part is in the main chain and the other part in the side chain) to the macromolecular chain of one aromatic polyimide, will keep and improve some properties of polyimide and will bring special properties of azobenzene moieties.

Thus, in this paper we present a series of azo-copolyimides obtained by solution polycondensation reaction of hexafluoroisopropylidene-bis(phthalic) anhydride (6FDA) with a mixture of two aromatic diamines, one of them containing a pendent substituted azobenzene group. The basic characterization of these compound has been previously reported by us.³⁷ However, in this work the azo-copolyimides were examined with respect to their dynamo-mechanical and dielectric properties, and the effect of the chemical structure of polymers on the physical properties are also discussed. Finally, the structuring polymer properties due to the presence of substituted azobenzene groups were investigated. The behaviour to structuring under laser beams of the free standing films from these azo-copolyimides was investigated in different conditions. It was believed that these complementary data would enable us to get better understanding of the respective structure – property relationships required for the development of high performance polymers.

2. Experimental part

2.1. Materials

N-methylpyrrolidinone (NMP) from Merck was dried on P₂O₅ and freshed distilled at reduced pressure. *para*-Toluidine, *meta*-phenylenediamine, acetic anhydride and pyridine were provided from different commercial sources (Fluka, Aldrich) and used as received.

2.2. Monomers

Aromatic diamines containing two ether bridges, namely 1,3-bis(*p*-aminophenoxy)benzene, 1,4-bis(*p*-aminophenoxy)benzene and 4,4'-bis(*p*-aminophenoxy)biphenyl, have been provided from different commercial sources and purified by recrystallization from ethanol or from a mixture of ethanol with water. M. p. 114-116°; 163-165°C and 197-199°C, respectively.

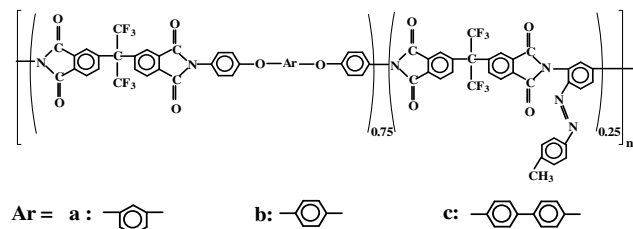
Aromatic diamine which has side substituted azobenzene group, namely 2,4-diamino-4'-methylazobenzene was synthesized via one-step diazonium coupling reaction of *para*-toluidine diazonium chloride with *meta*-phenylenediamine, as was previously reported.²⁶ ¹H NMR (DMSO-d₆): 2.34 ppm (CH₃), 5.84-5.90 ppm (NH₂), 6.00-6.036 ppm (Ar-H); 7.23-7.61 ppm (Ar-H); IR (KBr): 3470-3380 cm⁻¹ (-NH₂), 2900 cm⁻¹ (CH₃); UV-Vis (DMF): λ_{max} = 445 nm.

C₁₃H₁₄N₄ (226); Calcd. C 69%; H% 6.24; N% 24.76%; Found C 68.86%; H% 6.04; N% 24.33%; M.p: 145-146°C.

Hexafluoroisopropylidenediphthalic dianhydride (6FDA) from Hoechst – Celanese were purified in our laboratory by recrystallization from acetic anhydride. Melting point of 6FDA was 245-247°C.

2.3. Polymer synthesis

The structures of the azo-copolyimides studied in this paper are shown in the Scheme 1. These compounds have been synthesized by the polycondensation reaction of (hexafluoroisopropylidene)-diphthalic dianhydride and a mixture of two aromatic diamines, one of which contains ether groups, such as bis(*p*-aminophenoxy)-1,4-benzene, bis(*p*-aminophenoxy)-1,3-benzene or bis(*p*-aminophenoxy)-4,4'-biphenyl, and the other one contains a pendent substituted azobenzene group, namely 2,4-diamino-4'-methylazobenzene. The molar ratio between the two diamines is 0.75 : 0.25, respectively. The polycondensation reaction of these monomers was carried out by using a procedure reported previously.^{27,37}



Scheme 1. Structure of azo-copolyimides a – c

2.4. Measurements

FTIR spectra were recorded with a FT-IR VERTEX 70 (Bruker Optics Company), with a resolution of 0.5 cm^{-1} , by using KBr pellets or very thin polymer films.

Model molecules for a polymer fragment were obtained by molecular mechanics (MM+) by means of the Hyperchem program, Version 7.5.³⁸

The thermogravimetric analyses (TGA) were performed on a Mettler Toledo TGA-SDTA851e derivatograph. The data recording occurred in 20 mL/min out flow nitrogen, within 25-900 °C temperature range at a heating rate of 10°C/min. The test samples weighed 3-5 mg.

Dielectric parameters and molecular relaxations were characterized in broad temperature and frequency range by dielectric relaxation spectroscopy (DRS) using Novocontrol Dielectric Spectrometer. Dielectric measurements were run at constant temperature by taking frequency scans (1 Hz to 1 MHz) every 5°C between -120°C and + 250 °C. Measurements were made in a nitrogen atmosphere and the amplitude of AC applied voltage was 1 V. Silver electrodes with 20 mm diameter were painted on both samples surfaces to assure a good ohmic contact. Polyimide films with thicknesses comprised between 30 and 50 μm were placed between two round electrodes and tested. Without removing the polymer film from the measuring cell, a second measurement cycle was performed.

The radiation corresponding to the third harmonic of a pulsed Nd:YAG laser (Brilliant B from Quantel, 355 nm wavelength, 6 ns pulse duration, 6 mm in diameter) was used to generate an interference field in the near field of a phase mask (1000 grooves per mm). The incident fluency was 10 mJ/cm^2 and 45 mJ/cm^2 . The number of laser pulses was 10 and 100. The interference image that is produced in the near field is a periodical structure with the pitch of the same order of magnitude as that of the phase mask.³⁹ Polymers samples (1 cm x 1 cm) were mounted in an assembly sketched in Figure 1, and then exposed to the laser radiation interference field.

Single-frequency dynamic mechanical analysis (DMA) tests were conducted on a PerkinElmer Diamond instrument, in tension mode, on films with the length of 10 mm, width of 10 mm and thickness in the range of 0.04-0.06 mm. The single frequency temperature experiment was run by increasing the temperature in ramp mode with 2 °C/min, at 1 Hz, from -50 °C

until the temperature whereon the E' value was too low to allow the experiment to be continued.

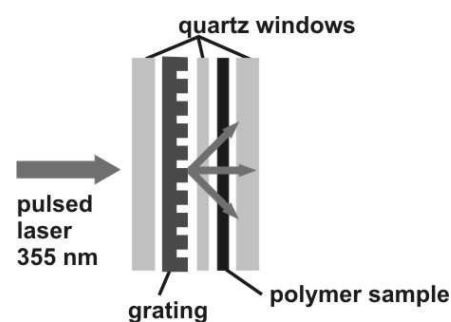


Fig. 1 The assembly used to irradiate azo-copolyimide films in pulsed laser radiation interference field.

The Atomic Force Microscopy investigations were done using a Scanning Probe Microscope Solver PRO-M apparatus (NT-MDT, Zelenograd, Russia). The film topography was analyzed in *tapping mode*, in air, using a rectangular cantilever NSG10/Au (NT-MDT, Zelenograd, Russia) with a nominal elasticity constant $k_N = 11.5\text{ N/m}$. Different scan sizes were analyzed by means of Nova v.1.26.0.1443 for Solver software, but the morphological features were easily observed when the scan length of 10 μm was utilized. From three-dimensional topographic data measurements, a spatial texture parameter, texture direction index (*Stdi*), which describes the orientation of structuring, was calculated based on the Fourier spectrum.⁴⁰

3. Results and discussions

3.1. General characterization

The structure of azo-copolyimides was identified by FTIR spectra. The presence of absorption bands characteristic for carbonyl group of the imide ring at about 1770-1780 and 1715-1725 cm^{-1} , and the characteristic band for C-N vibration at 1370-1385 and 720-730 cm^{-1} prove the formation of imide rings. All the copolyimides exhibit characteristic absorption bands of hexafluoroisopropylidene at 1240 cm^{-1} and 1100 cm^{-1} .^{22,37} The absorption band of the N=N linkage overlaps with that of C=C vibration of the benzene ring at about 1600 cm^{-1} . The strong absorption bands at 1230-1240 cm^{-1} were linked to the presence of aromatic ether bridges. C-H and C-C linkages in aromatic rings showed absorption peaks around 3100 cm^{-1} and 1490-1500 and 1595-1600 cm^{-1} . A typical FTIR spectrum is showed in Fig. 2.

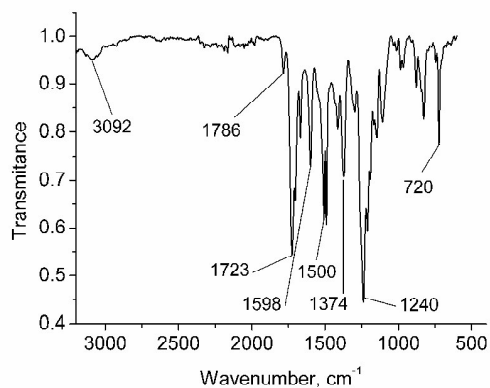


Fig. 2 FTIR Spectrum of the azo-copolyimide **b**

All polymers are easily soluble in NMP and other polar amide solvents such as dimethylsulfoxide (DMSO), dimethylformamide (DMF), dimethylacetamide (DMAc). These polymers are also soluble in less polar solvents like tetrahydrofuran (THF) and chloroform (CHCl₃). This good solubility is due to the presence of side azobenzene groups which increase the free volume and thus the close packing of the macromolecular chains is loose, allowing for the small solvent molecules to penetrate more easily among the polymer chains. Also, the hexafluoroisopropylidene and ether groups introduce more flexibility and that prevents a dense packing of the chains.^{27,37}

As it is shown in molecular models (Fig. 3), the shape of the macromolecular chains of these polymers is different from that of linear rigid rod which characterizes the completely insoluble aromatic polyamides or polyimides. This shape obstructs the dense packing of the macromolecules and the small solvent molecules can diffuse more easily between the polymer chains and thus leads to a better solubility.

All the synthesized copolymers possess good film-forming ability. The polymer solutions (15 %) in DMAc were processed into thin films by casting onto glass plates. The free-standing films having a thickness in the range of 10-30 μm were flexible, tough and non-creasable, and maintained their integrity after repeated bendings. The traces of the solvent were removed by Soxhlet extraction with methanol for 8 h and then the polymer films were characterized.

3.2. Thermal stability

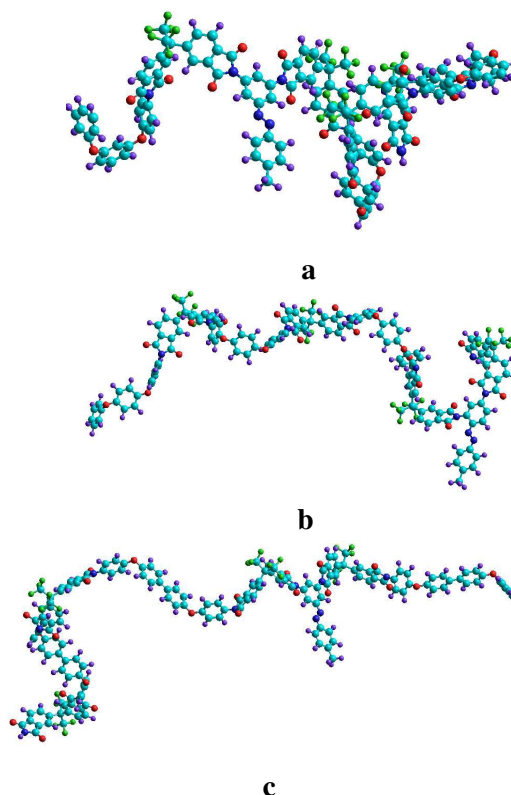


Fig. 3 Molecular models of azo-copolyimides **a**, **b** and **c** (one structural unit).

The thermal behavior of these polymers was investigated by thermogravimetric analysis. The thermogravimetric (TG) curves of copolyimides are shown in Fig. 4. The thermogravimetric and derivative thermogravimetric curves revealed that a very small quantity of solvent traces (0.2-0.3%) were removed at temperature around 200°C.

The thermal decomposition of all polymers is not complete at 900°C, as the remaining residue amounts in the range of 53.5-57.5 %. All the polymers under investigation revealed a very good thermal stability, as the thermal degradation onset temperature was above 300°C. The presence of the azo groups determines the first step of degradation at a temperature range of 305-325°C.³⁷ A very recent paper reported the similar thermal stability of an azopolyimide obtained from 6FDA and 2,4-diamino-4'-methylazobenzene.⁴¹ The weight loss due to the degradation of azo groups is 3.04 – 4.16%. The second step starts at about 500-510°C, ends at 577-587°C and is characterized by DTG peak at about 550°C. This step involves 19-22 % weight loss and represents the main decomposition process.

This last step can be attributed to the degradation of macromolecular chains of the polymer. As it can be seen,

hexafluoroisopropylidene groups preserve the thermal stability characteristic to wholly aromatic polyimides.

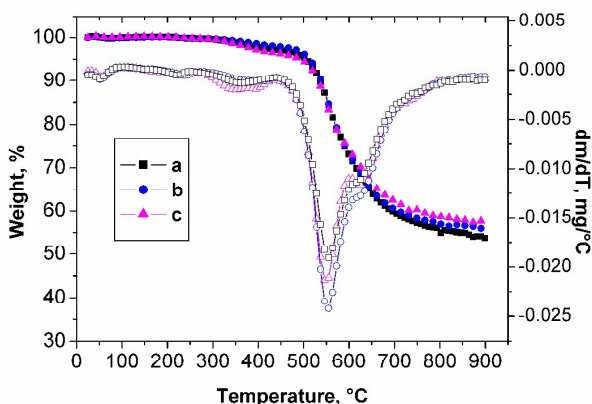


Fig. 4 TG-DTG curves of the azo-copolyimides **a-c**

3.3. Dynamo-mechanical analysis

Azo-copolyimide films show a high modulus, over 10^9 Pa, below its glass transition temperature (T_g), followed by a drastic drop in magnitude in the range of 140-185°C. The severe decrease in modulus with temperature indicates distinct transition from glassy to rubbery state which is the onset of the glass transition temperature.⁴² Thus, in the case of azo-copolyimide **a** which contains in the macromolecular chain more flexible units (the *meta*-catenated phenylene rings) the obtained value for α transition was lower than the value observed for the polymer **b** which has only *para*-catenated phenylene rings, being 146°C and 167°C, respectively. The presence of biphenyl units in the macromolecular chain of polymer **c** led to the highest value of α transition being 169°C. From the peaks of loss modulus it can be observed that the obtained values are slightly higher being 157°C, 176°C and 181°C, for azo-copolyimides **a**, **b** and **c**, respectively (Fig. 5a). As the glass transition process advances, it becomes more than a coordinated molecular motion of macromolecular segments, that start to slip one past another. This fact determines the rapid increase of $\tan \delta$ with temperature in the second part of the glass transition, therefore the $\tan \delta$ peak is faded and it is turned into a shoulder for polymers **a** and **b** or it is totally hidden in the case of the polymer **c** (Fig. 5b).

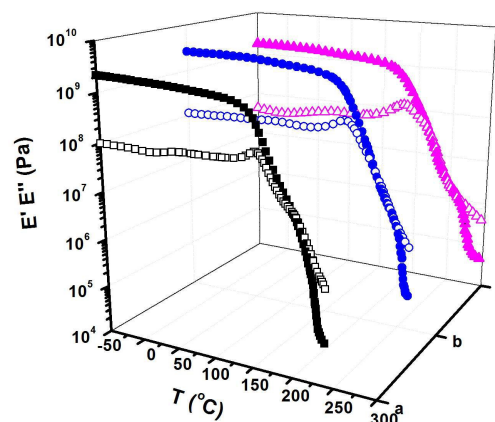


Fig. 5a Temperature dependence of the storage modulus (solid symbols) and loss modulus (open symbols) for azo-copolyimide films **a-c**.

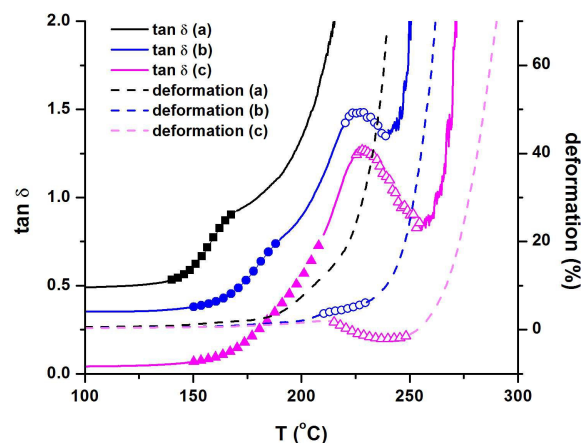


Fig. 5b Temperature dependence of the loss factor and deformation for azo-copolyimide films **a-c**.

For the sake of clarity the $\tan \delta$ curves were shifted vertically, without modifying any characteristics. In the representation the increasing side of $\tan \delta$ peak during the glass transition is marked with solid symbols. Further on the evolution of $\tan \delta$ with temperature is practically the result of the polymer structure on the viscoelastic behaviour. The evolution of the sample length during the DMA experiment, displayed as deformation in Fig. 5b, can offer also an indication of the phenomena that takes place.⁴³ Polymer **a**, the most flexible, registers a continuous increase of the sample length that comes along with the constant increase of $\tan \delta$ with temperature until the end of the experiment. Polymers **b** and **c** have particular behaviours generated by the effect of their structures. The presence of *p*-phenylene and *p*-diphenylene rings in their structures makes possible, under adequate conditions, the

appearance intermolecular associations through the π - π interactions between the aryl rings. The extra-mobility earned by the macromolecular chains subjected to tension, after the glass transition, induces chain arrangements favourable for intermacromolecular π - π interactions. In these conditions the rigidity of the polymers **b** and **c** increases and, accordingly, $\tan \delta$ decreases. This moment is marked on $\tan \delta$ curves with open circles (polymer **b**) and open triangles (polymer **c**). The effect is stronger for the polymer **c** with p-diphenylene rings, where the deformation of the sample registers even a contraction (the region marked with open triangles on the deformation curve) and not only a stagnation of the elongation as for the polymer **b** (the region marked with open circles on the deformation curve). Over 200 °C these interaction are not anymore so strong and the flowing phenomena take over. However, the films keep their load-bearing properties until low values of E' modulus, under 10^5 Pa due to the intermacromolecular interactions.

3.4. Dielectric properties

Dielectric relaxation spectroscopy provided information about the storage and dissipation components of the complex permittivity, namely dielectric constant (ϵ') and dielectric loss (ϵ''), of the polyimide films in broad frequency and temperature range. Also, from their variation, thermal transitions correlated with dipolar movements are evidenced.

As reported for other polyimides,⁴⁴⁻⁴⁶ and generally for polymers, dielectric constant, ϵ' , decreases with increasing frequency for the investigated copolyimides (Fig. 6). The dielectric constant being dependent on the ability of polarizable units to align to the alternating electric field, it decreases with increasing frequency since the orientation of dipole moments needs longer time than that corresponding to applied frequency.

It is well-known that polymers which contain hexafluoroisopropylidene (6F) groups have dielectric constants with the lowest values. This is due to hydrophobic character of 6F which translates into minimal absorption of polar water molecules and on the other hand, to the lower polarizability of the fluorinated chains. The polarizability of the system is low for two reasons: first, the hexafluoroisopropylidene group induces a low electronic polarizability due to the electron-withdrawing effects^{46,47} and secondly, it decreases the polarizability per volume unit by increasing the free volume due the steric hindrance effects of 6F which impedes a closer molecular packing of the polymer

chains. Consequently, polymers which incorporate two symmetric CF_3 groups present lower dielectric constants, as it was also observed by other authors.⁴⁸

In the case of these azo-copolyimides the introduction of azobenzene group and hexafluoroisopropylidene units in the same macromolecular chain led to lower values of dielectric constants for azo-copolyimides **a** and **b** (3.43 and 3.25, respectively) and a value close to that one of Kapton film for polymer **c** (3.65). The Kapton film, is the most common polyimide used as dielectric in advanced microelectronic applications and presents a dielectric constant of 3.5.⁴⁹ As can be seen in Fig. 6, the dielectric constant varies little with temperature in the range of $-100^\circ\text{C} \div +135^\circ\text{C}$ for azo-copolyimide **a** and till $+155^\circ\text{C}$ for azo-copolyimides **b** and **c**. A sharply increase of the dielectric constant for polymer **a** was observed after 135°C and a moderately one for the other polymers (**b** and **c**).

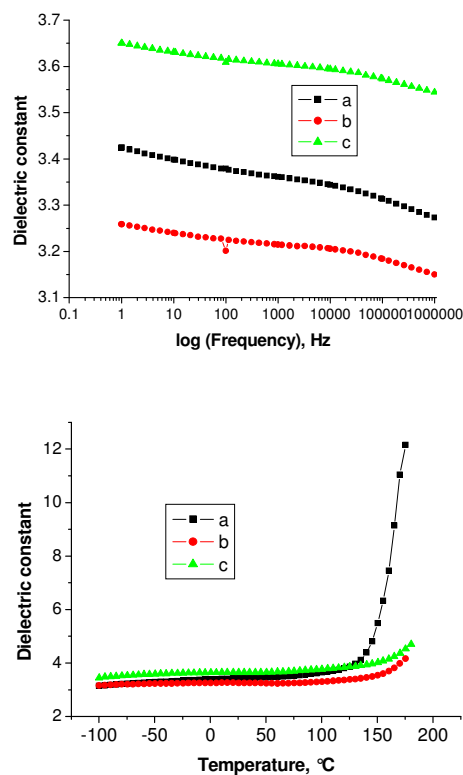


Fig. 6 Dielectric constant vs frequency at 25 °C (up) and dielectric constant vs temperature at 1 Hz (down), for azo-copolyimides **a-c**.

This can be explained by the higher flexibility of the azo-copolyimides **a**, with *meta*-catenated phenylene group in the macromolecular chain, which led to the mobility of the charge carriers.⁴⁵

Fig. 7 a - d shows the three-dimensional frequency and temperature dependencies of the dielectric constant and dielectric loss for azo-copolyimide film **a**, from the first and the second measurements. The other measured films have similar trends. In the negative temperature region of the dielectric loss representations, γ relaxation peak appears around $-100\text{ }^{\circ}\text{C}$ at 1 Hz and shifts to higher temperatures with increasing frequency, up to around $20\text{ }^{\circ}\text{C}$ for 1 MHz . For polyimide films γ transition has been associated with phenyl ring oscillations and is influenced by moisture absorption content.⁵⁰ In $50 - 150\text{ }^{\circ}\text{C}$ temperature range, β relaxation appears as a shoulder because of overlapping with γ relaxation at high frequencies and low temperature, and with losses caused by increased conductivity especially at high temperature and low frequencies. Starting around $130\text{ }^{\circ}\text{C}$, correspondingly to the increase of ϵ'' , there is a sharp increase in ϵ' at low frequencies, due to the increased mobility of charges that accumulate at the interfaces between regions of different electrical and dielectric properties.

In the second measurement the dielectric constant was slightly decreased (with about 0.2) and γ relaxation disappeared (Figs. 7d and 8). This observation suggests that the process is related to the movement of less polar groups, the molecular movement being evidenced by its coupling with that of polar molecules, most probably absorbed water molecules, which served as markers and are removed during the first heating cycle. This effect is highlighted in Fig. 8, where dielectric data recorded isothermally have been replotted as ϵ'' versus temperature at 1 kHz (Fig. 8).

As can be seen all the azo-copolyimides showed γ relaxation around $-50\text{ }^{\circ}\text{C}$ at 1 kHz , with slightly lower temperature for **b** copolymer. Beside the extinction of γ process, in the second measurement there is a small decrease of ϵ'' and also a less pronounced conductivity effect, which permits a better visualization of β relaxation. Regarding β relaxation, detailed studies on the molecular dynamics of polyimides have shown that it is determined by the mobility in the dianhydride group⁵⁰ which may include correlated movement of larger portions of the structural unit,⁵¹ or even the whole repeating segment for more rigid systems.⁵²

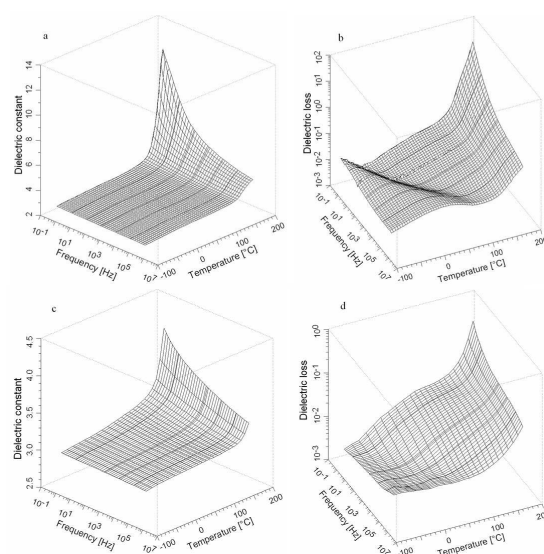


Fig. 7 Frequency and temperature dependencies of dielectric constant and dielectric loss from the first (a and b) and second (c and d) measurement for azo-copolyimide film **a**.

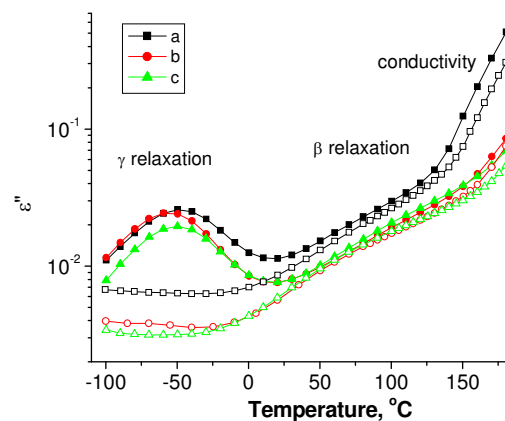


Fig. 8 Temperature dependence of dielectric loss, ϵ'' , at 1 kHz : full symbols – first heating; empty symbols–second heating cycle.

In order to determine the relaxation time, τ_{max} for γ relaxations, each relaxation peak in frequency domain, $\epsilon''(f)$, was analyzed by fitting the measured data to the empirical Havriliak-Negami (HN) function⁵³ and for β relaxations by fitting $\epsilon''(f)$ to a sum of a HN function for the dipolar relaxation and an exponential term for the conductivity contribution at low frequency.⁵⁴ For both secondary relaxations, Arrhenius temperature dependencies were obtained for the relaxation times:

$$\tau_{max}(T) = \tau_0 \exp\left(\frac{E_a}{kT}\right)$$

where E_a is the apparent activation energy of the process, k – Boltzmann's constant, τ_0 – the preexponential factor and represents the relaxation time at very high temperature.

Using Arrhenius representation (Fig. 9), activation energies for γ and β transitions were determined. The γ relaxation E_a of 48.5 kJ/mol for **a**, 45.2 kJ/mol for **b** and 45.5 kJ/mol for **c** agrees reasonably well with the value of 43 kJ/mol reported for Matrimid polyimide.⁵⁵ Activation energies characteristic of β relaxation are in the range of 98.5-134 kJ/mol, and is similar to the calculated values for other polyimide structures 95 ÷ 180 kJ/mol.^{56,57}

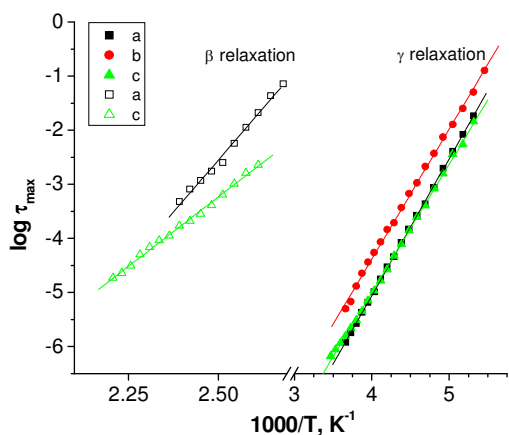


Fig. 9 Arrhenius plot of $\log(\tau_{max})$ vs. $1000/T$ for secondary relaxation

As typical for polyimides without pendent groups,^{50,54} only two subglass transitions were observed for the investigated samples. This indicates that for investigated temperature range, there is no dielectric relaxation corresponding to movement of the lateral chain that includes azo chromophores and that, during the repeated heating up to +180 °C, no configuration change of the

lateral group take place. Probably for this temperatures the main chain rigidity and the molecular packing does not allow any configuration or conformation change of the lateral group.

3.5. The surface structuring investigations

Taken into account that all investigated samples showed good thermal stability and low dielectric constant, these thin azo-copolyimide films may be used in high performance applications, namely stable photonic structures (for one- and two-dimensional linear diffraction gratings, spectral filters, subwavelength gratings, near-field sensing and imaging instruments) or long-term optical devices (for storage, processing, displaying, and transfer of optical information). For this purpose, we have studied the possibility to obtain tridimensional surface relief structuration by laser irradiation.

The investigation of surface structuring capacity demonstrated that the irradiation conditions have a prominent influence on surface geometry of the polymers.^{32,58,59} Surface irradiation was realised under the action of a laser field with a controlled distribution represented by an interference pattern. The light source of our setup was a Nd:YAG laser working on his third harmonic at 355 nm and with a pulse length at FWHM (full width half maximum) of 6 ns.

Atomic force microscopy was used to characterize the resulted structured surfaces. In order to describe the preferential orientation of the surface morphology, the texture direction index ($Stdi$) was used. Surfaces with very dominant directions have $Stdi$ values close to zero and those with no texture orientation have $Stdi$ close to 1. As can be seen in Fig. 10, by using an energy density of 10 mJ/cm² and 10 pulses, the obtained surface photoinduced pattern is well defined in the case of azo-copolyimides **a** and **c** and uneven for polymer film **b**. This fact is also argued by the values of $Stdi$, which were 0.303 and 0.232 for **a** and **c** copolyimides, indicating a good anisotropy of the morphology and slightly higher (0.529) for polymer film **b**, showing a mild texture orientation. The pattern depth has values in the range 30-100 nm.

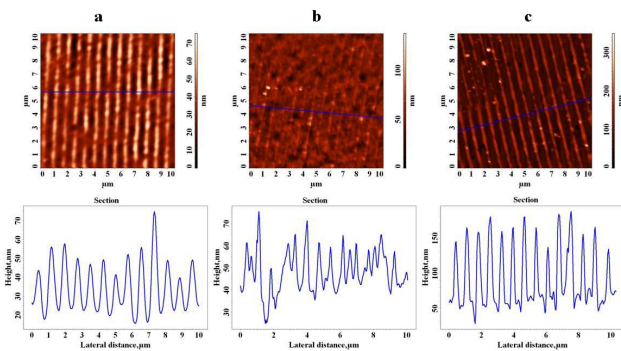


Fig. 10 AFM images of the structured surface and corresponding cross-section profiles of azo-copolyimide films **a-c** after irradiation with 10 mJ/cm^2 by using 10 pulses.

5

Applying 100 pulses, the surface relief became even and uniform in the case of polymer films **b** and **c**, with a pattern depth of about 100-150 nm (Fig. 11). The texture direction index values close to zero (0.295 for film **b** and 0.252 for film **c**) confirm this statement. By increasing the pulse number, the accuracy of the surface relief definition is diminished in the case of compound **a** (Fig. 11a), probably due to some supplementary modulation effects. In this case, an increase of the *Stdi* from 0.303 (10 mJ/cm^2 ; 10 pulses) to 0.546 (10 mJ/cm^2 ; 100 pulses) was observed, pointing out that the surface anisotropy has decreased considerably.

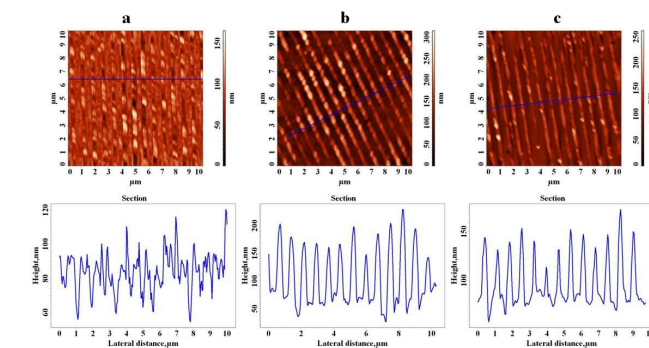


Fig. 11 AFM images of the structured surface and corresponding cross-section profiles of azo-copolyimide films **a-c** after irradiation with 10 mJ/cm^2 by using 100 pulses.

20

By increasing the radiation energy density to 45 mJ/cm^2 it was observed that the surface photoinduced pattern had a similar appearance, as in the case previously showed for azo-copolyimides **b** and **c** (Fig. 12). For samples **b** and **c** where it was applied 10 pulses, the pattern depth of about 120-140 nm was obtained and surface photoinduced pattern was very well-defined and the generated channels were even and uniform. *Stdi* of 0.197

25

(for sample **b**) and 0.261 (for sample **c**) denote stronger anisotropy, the surfaces having oriented and periodic structures.

30

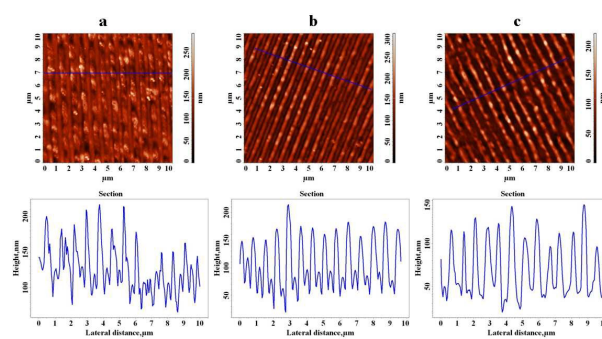
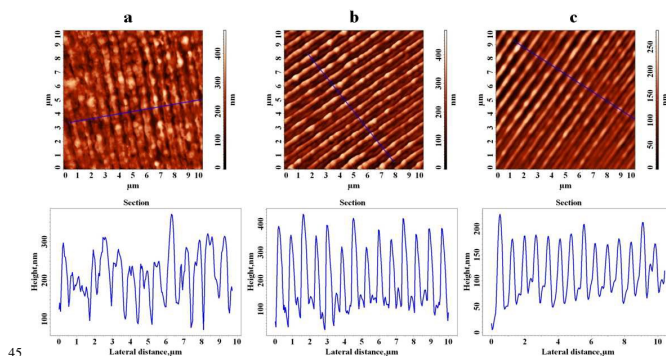


Fig. 12 AFM images of the structured surface and corresponding cross-section profiles of azo-copolyimide films **a-c** after irradiation with 45 mJ/cm^2 by using 10 pulses.

35

When the number of pulses was increased, the surface relief became much more regular (Fig. 13 **b, c**). The maximum pattern depth, which has been obtained in these cases, were 240 nm for 100 subsequent irradiation pulses for polymer samples **b** and **c** around 200 nm for azo-copolyimide **c**. The high degree of surface orientation was confirmed in the case of polymer films **b** and **c** by *Stdi* values of 0.211 and 0.195, respectively, and a mild degree of surface orientation for polymer film **a** which presented a *Stdi* value of 0.437.



45

Fig. 13 AFM images of the structured surface and corresponding cross-section profiles of azo-copolyimide films **a-c**, after irradiation with 45 mJ/cm^2 by using 100 pulses.

By analyzing a profile diagram it can be observed that the homogeneity of the surface features is satisfactory, the deviations being in the domain of 40-50 nm. For polymer samples **a** the irregular surface relief was maintained with an average pattern depth about 180 nm (Fig. 10 **a**).

55

As can be seen in the AFM images presented in Figs. 10-13, the azo-copolyimide film **a** showed an irregular surface

photoinduced pattern for high energy fluency (45 mJ/cm^2) and for 100 pulses and low energy fluency (10 mJ/cm^2). This can be explained by slightly higher flexibility of the polymer chain **a**, which contains *meta*-catenated linkages, compared with polymers **b** and **c**, which have only *para*-catenated linkages. The photoinduced pattern was generated in this polymer, but the surface relief grating could not be fixed well, because of the fairly high mobility of the polymer chain which tends effectively to relax to a smooth surface due to surface tension forces.⁶⁰ Regarding the mechanism of the surface structuring it can be suggested that this process takes place by surface reorganization, based on consideration that the irradiation conditions consist of very short exposure time.²⁹

4. Conclusions

The introduction of pendent substituted azobenzene units together with hexafluoroisopropylidene bridges into the chain of aromatic polyimides determined the obtaining of polymers with remarkable solubility in polar amide solvents such as NMP and DMF, and even in less polar solvents like THF or CHCl_3 . The good solubility makes the present copolyimides potential candidates for applications in spin coating and casting processes. All the azo-copolyimide films showed a high modulus, over 10^9 Pa , below the glass transition temperature. The dielectric constant of azo-copolyimide films were in the range of 3.25-3.65 at room temperature and 1 Hz. All azo-copolyimide films showed γ transition around -50°C at 1 kHz, with activation energy in the range of 45-48 kJ/mol.

All investigated polymers showed good thermal stability with initial decomposition temperature above 300°C . Free-standing films were obtained and the structuring capacity was investigated by using two laser fluency 10 mJ/cm^2 and 45 mJ/cm^2 with 10 and 100 pulses number. The best results were obtained by using high density energy (45 mJ/cm^2) for azo-copolyimides with *para*-catenated units (**b** and **c**). The uniform surface relief grating was obtained with a maximum photoinduced pattern depth of 240 nm for polymer **b** by using an energy fluency of 45 mJ/cm^2 and 100 pulses. These results were also argued by the texture direction parameter, which indicates in this case a good anisotropy of the morphology.

Acknowledgements

The work has been funded by the Sectoral Operational Programme Human Resources Development 2007-2013 of the Ministry of European

Funds through the Financial Agreement POSDRU/159/1.5/S/132397 and by the European Union's Seventh Framework Programme (FP7/2007-2013) under grant agreement n°264115 - STREAM. The POSCCE-O 2.2.1, SMIS-CSNR 13984-901, No. 257/28.09.2010 Project, CERNESIM, is also gratefully acknowledged for the infrastructure used in this work.

References

- G. S. Kumar and D.C. Neckers, *Chem. Rev.*, 1989, **89**, 1915-1925.
- A. Natansohn and P. Rochon, *Chem. Rev.*, 2002, **102**, 4139-4176.
- S. K. Yeshoda, Ch. K. S. Pillai and N. Tsutsumi, *Prog. Polym. Sci.*, 2004, **29**, 45-74.
- E. Hamciuc, I. Sava, M. Bruma, T. Kopnick, B. Schulz, B. Sapich, J. Wagner and J. Stumpe, *Polym. Adv. Technol.*, 2006, **17**, 641-646.
- I. Sava, M. Bruma, Th. Köpnick, B. Schulz, B. Sapich, J. Wagner and J. Stumpe, *High Perform. Polym.*, 2007, **19**, 296-310.
- Q. Ferreira, P.A. Ribeiro, O.N. Oliveira Jr and M. Raposo, *Appl. Mater. Interfaces*, 2012, **4**, 1470-1477.
- H.-Y. Huang, Jh.-W. Jian, Y.-T. Lee, Y.-T. Li, T.-Ch. Huang, J.-H. Chang, L.-Ch. Yeh and J.-M. Yeh, *Polymer*, 2012, **53**, 4967-4976.
- D. Wang and X. Wang, *Prog. Polym. Sci.*, 2013, **38**, 271-301.
- R. Fernández, I. Mondragon, R.C. Sanfelice, F.J. Pavinatto, O.N. Oliveira Jr., P. Oyanguren and M.J. Galante, *Mater. Sci. Eng.*, 2013, **C 33**, 1403-1408.
- L. Nedelchev, D. Nazarova and V. Dragostinova, *J. Photoch. Photobiol.*, 2013, **A 261**, 26-30.
- D.Y. Kim, S.K. Tripathy, L.Li and J. Kumar, *Appl. Phys. Lett.*, 1995, **66**, 1166-1168.
- Y. Wu, A. Natansohn and P. Rochon, *Macromolecules*, 2004, **37**, 6090-6095.
- T. Fukuda, J. Y. Kim, D. Barada and K. Yase, *J. Photochem. Photobiol. A: Chem.*, 2006, **183**, 273-279.
- P. Rochon, E. Batalla and A. Natansohn, *Appl. Phys. Lett.*, 1995, **66**, 136-138.
- M.K. Ghosh, K.L. Mittal (Eds.), *Polyimides: Fundamentals and Applications*, Marcel Dekker Inc., New York, 1996.
- H.L. Lin, T.-Y. Juang, L.-H. Chan, R.-H. Lee, S.A. Dai, Y.-L. Liu, W.-C.h. Su and R.-J. Jeng, *Polym. Chem.*, 2011, **2**, 685-693.
- C. Wang, W. Chen, Y. Chen, X. Zhao, J. Li and Q. Ren, *Mater. Chem. Phys.*, 2014, **143**, 773-778.
- O. Yaroshchuk and Y. Reznikov, *J. Mater. Chem.*, 2012, **22**, 286-300.
- Y. Yu, M. Nakano, A. Shishido, T. Shiono and T. Ikeda, *Chem. Mater.*, 2004, **16**, 1637-1643.
- D. H. Wang, K.M. Lee, Z. Yu, H. Koerner, R.A. Vaia, T. J. White and L.-S. Tan, *Macromolecules*, 2011, **44**, 3840-3846.
- K. M. Lee, D. H. Wang, H. Koerner, R. A. Vaia, L.-S. Tan and T. J. White, *Angew. Chem. Int. Ed.*, 2012, **51**, 4117-4121.
- N. Hosono, M. Yoshikawa, H. Furukawa, K. Totani, K. Yamada, T. Watanabe and K. Horie, *Macromolecules*, 2013, **46**, 1017-1026.
- E. Schab-Balcerzak, L. Grobelny, A. Sobolewska and A. Miniewicz, *Eur. Polym. J.*, 2006, **42**, 2859-2871.

24. E. Schab-Balcerzak, A. Sobolewska and A. Miniewicz, *Opt. Mater.*, 2008, **31**, 405-411.
25. E. Schab-Balcerzak, M. Siwy, M. Kawalec, A. Sobolewska, A. Chamera and A. Miniewicz, *J. Phys. Chem. A*, 2009, **113**, 8765-8780.
26. E. Schab-Balcerzak, B. Sapich and J. Stumpe, *Polymer*, 2005, **46**, 49-59.
27. I. Sava, A.M. Resmerita, G. Lisa, V. Damian and N. Hurduc, *Polymer*, 2008, **49**, 1475-1482.
28. M. Siwy, B. Jarzabek, K. Switkowski, B. Pura and E. Schab-Balcerzak, *Polym. J.*, 2008, **40**, 813-824.
29. I. Sava, L. Sacarescu, I. Stoica, I. Apostol, V. Damian and N. Hurduc, *Polym. Int.*, 2009, **58**, 163-170.
30. E. Schab-Balcerzak, H. Janeczek and P. Kucharski, *J. Appl. Polym. Sci.*, 2010, **118**, 2624-2633.
31. E. Schab-Balcerzak, M. Siwy, B. Jarzabek, A. Kozanecka-Szmigiel, K. Switkowski and B. Pura, *J. Appl. Polym. Sci.*, 2011, **120**, 631-643.
32. I. Sava, N. Hurduc, L. Sacarescu, I. Apostol and V. Damian, *High Perform. Polym.*, 2013, **25**, 13-24.
33. I. Sava, A. Burescu and B. Jarzabek, *High Perform. Polym.*, 2014, **26**, 73-80.
34. K. Sakamoto, K. Usami, M. Kikegawa and S. Ushioda, *J. Appl. Phys.*, 2003, **93**, 1039-1043.
35. T.V. Rajendiran and C. Anbuselvan, *Asian J. Chem.*, 2010, **22**, 4985-4995.
36. A. Georgiev, V. Strijkova, D. Dimov, E. Spassova, J. Assa and G. Danev, *Solid State Phenom.*, 2010, **159**, 141-144.
37. A. Burescu, I. Sava and M. Bruma, *Rev. Chim-Bucharest*, 2013, **64**, 1047-1050.
38. Hypercube Inc. (Ontario) 2002 Hyperchem Version 7.5.
39. M. C. Castex, C. Oliveiro, A. Fischer, S. Mousel, J. Michelin, D. Ades and A. Siove, *Appl. Surf. Sci.*, 2002, **197-198**, 822-825.
40. G. Barbato, K. Carneiro, D. Cuppini, J. Garnaes, G. Gori, G. Hughes, C. P. Jensen, J. F. Jørgensen, O. Jusko, S. Livi, H. McQuoid, L. Nielsen, G. B. Picotto and G. Wilkening, Scanning tunneling microscopy methods for roughness and micro hardness measurements, Synthesis report for research contract with the European Union under its programme for applied metrology, (1995) 109 pages European Commission Catalogue number: CD-NA-16145 EN-C, Brussels, Luxemburg.
41. E. Schab-Balcerzak, B. Skorus, M. Siwy, H. Janeczek, A. Sobolewska, J. Konieczkowska and M. Wiacek, *Polym. Int.*, 2015, **64**, 76-87.
42. I. Sava, S. Chisca, M. Bruma, G. Lisa, *J. Therm. Anal. Calorim.*, 2011, **104**, 1135-1143
43. M. Cristea, D. Ionita, C. Hulubei, D. Timpu, D. Popovici and B. C. Simionescu, *Polymer*, 2011, **52**, 1820-1828.
44. I. Sava, M. Bruma, C. Hamciuc, E. Hamciuc, D. Timpu and F. Mercer, *J. Appl. Polym. Sci.*, 2001, **80**, 650-657.
45. I. Sava, M.D. Iosip, M. Bruma, C. Hamciuc, J. Robison, L. Okrasa and T. Pakula, *Eur. Polym. J.*, 2003, **39**, 725-738.
46. I. Sava, S. Chisca, M. Bruma and G. Lisa, *Polym. Bull.*, 2010, **65**, 363-375.
47. S. Chisca, I. Sava, V. Musteata and M. Bruma, *Eur. Polym. J.*, 2011, **47**, 1186-1197.
48. S.-U. Kim, C. Lee, S. Sundar, W. Jang, S.-J. Yang and H. Han, *J. Polym. Sci. B, Polym. Phys.*, 2004, **42**, 4303-4312.
49. M.D. Damaceanu, V.E. Musteata, M. Cristea and M. Bruma, *Eur. Polym. J.*, 2010, **46**, 1049-1062.
50. C. Bas, C. Tamagna, T. Pascal and N. D. Alberola, *Polym. Eng. Sci.*, 2003, **43**, 344-355.
51. Z. Sun, L. Dong, Y. Zhuang, L. Cao, M. Ding and Z. Feng, *Polymer*, 1992, **33**, 4728-4731.
52. K. L. Ngai and M. Paluch, *J. Chem. Phys.*, 2004, **120**, 857-873.
53. S. Havriliak and S. Negami, *J. Polym. Sci. Polym. Symp.*, 1966, **14**, 99-117.
54. M. D. Damaceanu, R. D. Rusu, V. E. Musteata and M. Bruma, *Soft Materials*, 2010, **9**, 44-63.
55. A.C. Comer, D.S. Kalika, B.W. Rowe, B.D. Freeman and D.R. Paul, *Polymer*, 2009, **50**, 891-897.
56. H. Deligoz, S. Ozgumus, T. Yalcinyuva, S. Yildirim, D. Deger and K. Ulutas, *Polymer*, 2005, **46**, 3720-3729.
57. L. Fuming, J. G. Jason, P. S. Honigfort, S. Fang, J. C. Chen, F. W. Harris and S. Z. D. Cheng, *Polymer*, 1999, **40**, 4987-5002.
58. L. Rosu, I. Sava and D. Rosu, *Appl. Surf. Sci.*, 2011, **257**, 6996-7002.
59. I. Stoica, L. Epure, I. Sava, V. Damian and N. Hurduc, *Microsc. Res. Tech.*, 2013, **76**, 914-923.
60. N.K. Viswanathan, D.Y. Kim, S. Bian, J. Williams, W. Liu, L. Li, L. Samuelson, J. Kumar and S.K. Tripathy, *J. Mater. Chem.*, 1999, **9**, 1941-1955.